Eur Biophys J (2011) 40:589–597
DOI 10.1007/s00249-011-0683-6

REVIEW

Almost lost in translation. Cryo-EM of a dynamic macromolecular complex: the ribosome

Mikel Valle

Received: 8 November 2010 / Revised: 31 January 2011 / Accepted: 3 February 2011 / Published online: 19 February 2011

Abstract Ribosomes are dynamic biological machines that perform numerous tasks during translation, the biosynthesis of proteins. Translocation, the movement of transfer RNAs (tRNAs) and messenger RNA (mRNA) to progress in the reading frame of codons in the mRNA, takes place after the addition of each amino acid. This process involves large ribosome conformational changes, where tRNAs proceed through intermediate states. The structural characterization of these translocation intermediates has remained elusive. Cryo-electron microscopy (cryo-EM) produces three-dimensional averages, and translocating ribosomes poise distinct conformational states, and hence, structurally heterogeneous populations. During the last decade, the quest for visualization of translocation intermediates has progressed together with the development of classification tools in cryo-EM. Some of these new tools have recently been tested in ribosomal translocation, uncovering a clearer picture of the process. This success goes along with the latest advances in cryo-EM and illustrates how the technique offers multiple possibilities for studying macromolecular complexes engaged in dynamic reactions.

M. Valle (✉)
Centre for Cooperative Research in Biosciences,
CICbioGUNE, Biscay Technology Park,
48160 Derio, Spain
e-mail: mvalle@cicbiogune.es

M. Valle
Department of Biochemistry and Molecular Biology,
University of the Basque Country, P.O. Box 644,
48080 Bilbao, Spain

Keywords Cryo-electron microscopy · 70S ribosome · Translocation · Classification · Hybrid tRNA

Introduction

Protein biosynthesis, also known as translation, takes place in ribosomes, large macromolecular complexes composed of ribosomal RNAs (rRNAs) and proteins. The mechanisms leading to the production of proteins involve several other elements, such as translation factors and tRNAs, which transiently interact with the ribosome. Together, ribosomes and their partners translate the genetic information coded in mRNA into a particular sequence of amino acids in the "language" of proteins. The ribosome is one of the largest macromolecular complexes in the cell, and its overall structure is conserved throughout all kingdoms of life, linked to the common nature of the process of protein synthesis. Understanding this multistep mechanism requires deep structure–function knowledge, and the current view of the dynamic ribosome machine has been enriched by contributions from several disciplines within structural biology (Ramakrishnan 2008; Steitz 2008). The first publications of atomic-resolved structures for bacterial ribosomes were landmarks for crystallographic studies (Ban et al. 2000; Schluenzen et al. 2000; Wimberly et al. 2000) and have defined the foundations on which current ribosome knowledge relies. Crystallography, however, depicts static pictures of ribosomes, and complementary techniques are needed to fully address their physiological functioning. In this regard, cryo-EM has profoundly contributed to understanding of ribosomes when crystal structures were not available (Frank et al. 1995) and in combination with crystallographic data to create pseudo-atomic models of ribosome dynamics (Mitra and Frank 2006).

The ribosome as seen by cryo-EM

Ribosomes are large complexes (70S particles from bacteria are around 2.5 MDa) that have a compact core of rRNA. They resemble spheres (around 250 Å in diameter for bacterial 70S ribosomes) bearing some protruding regions that increase the asymmetry of the complex. These ribosomal features fit the requirements of well-suited samples for cryo-EM. The dense core of rRNA produces high-contrast images for ribosomes embedded in a thin layer of amorphous ice (Fig. 1a). The two-dimensional (2D) images for ribosomes obtained in micrographs are isolated and processed as single particles (Fig. 1b) and represent projections of a three-dimensional (3D) object. The image processing for ribosomal samples (Frank et al. 2000) follows the projection-matching scheme, where experimental images are iteratively compared with a discrete library of projections ("prj_i" in Fig. 1c) obtained from a known initial 3D reference ("ref" in Fig. 1c). Each single image for a ribosomal particle is assigned to the in silico projection with highest cross-correlation, and the parameters associated with the simulated 2D image are then linked to the experimental particle. When all the images have gone through the comparison, a new 3D map is generated. The asymmetric structure of the ribosome generates easily distinguishable 2D views (class averages in Fig. 1d) which support efficient alignments between images.

After segmentation of the components and associated partners from 3D density maps, rendering of cryo-EM data for bacterial ribosomes depicts the 70S particle composed of two ribosomal subunits, the large (50S) and small (30S) subunits (Fig. 2), assembled by intersubunit bridges. There is an intersubunit space (Fig. 2b) where tRNAs bind to the A (aminoacyl), P (peptidyl), and E (exit) sites. The entrance and exit of this chamber have large protuberances with important regulatory and functional roles. In the entrance we find the base of the L7/L12 stalk ("Sb" in Fig. 2a, b), a binding site for most of the translation factors. Furthermore, this region contains elements that participate in the activation of the GTPase activity of translational GTPases. In the exit, the L1 stalk ("L1" in Fig. 2a, b) constructs a highly mobile region that is involved in interactions with tRNAs exiting the ribosome.

The structural separation of ribosomes into two subunits correlates with the division of fundamental functions in translation. Thus, "reading" of the genetic code information takes place in the small subunit between the anticodon of the incoming A-site tRNA and the codon in the mRNA in a region of the 30S subunit known as the decoding center ("dc" in Fig. 2c). In cryo-EM maps, the mRNA, a single-stranded nucleic acid, is not visible unless it interacts with other RNAs as in codon–anticodon pairing (with tRNAs) or with the helix constructed by the Shine–Dalgarno in the mRNA and the anti-Shine–Dalgarno in the 23S rRNA. The other main activity, the "writing" of the protein by sequential incorporation of amino acids, occurs in the large subunit at the peptidyl-transferase center ("PTC" in Fig. 2c), between the acceptor ends of A- and P-site tRNAs. The polypeptide being synthesized crosses the body of the 50S subunit through a peptide tunnel ("T" and red glowing conduit in Fig. 2c). In ribosomes programmed to synthesize long polypeptides, the protein can be detected by high-resolution cryo-EM within this channel (Seidelt et al. 2009). This division of labor is complemented by communication between ribosomal subunits, and the relative influence on their functioning travels through interconnecting bridges, tRNAs, and factors that bind to both subunits.

Translocation of tRNAs

Translation involves several steps, including elongation, the protein synthesis per se. During elongation, cognate aminoacyl-tRNAs (aa-tRNAs) are incorporated into the ribosome delivered by the elongation factor Tu (EF-Tu).

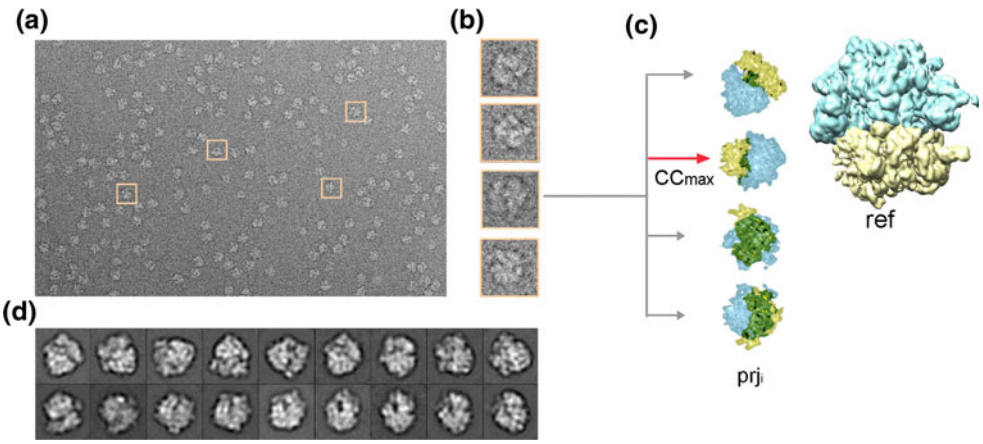

Fig. 1 70S ribosomes from *E. coli* observed by cryo-EM. Individual 70S particles are seen in a micrograph (**a**), from which single images are extracted (**b**) and compared with simulated projections produced by an initial reference (**c**). The highly asymmetric 70S ribosome generates distinguishable 2D images such as the class averages shown in (**d**)

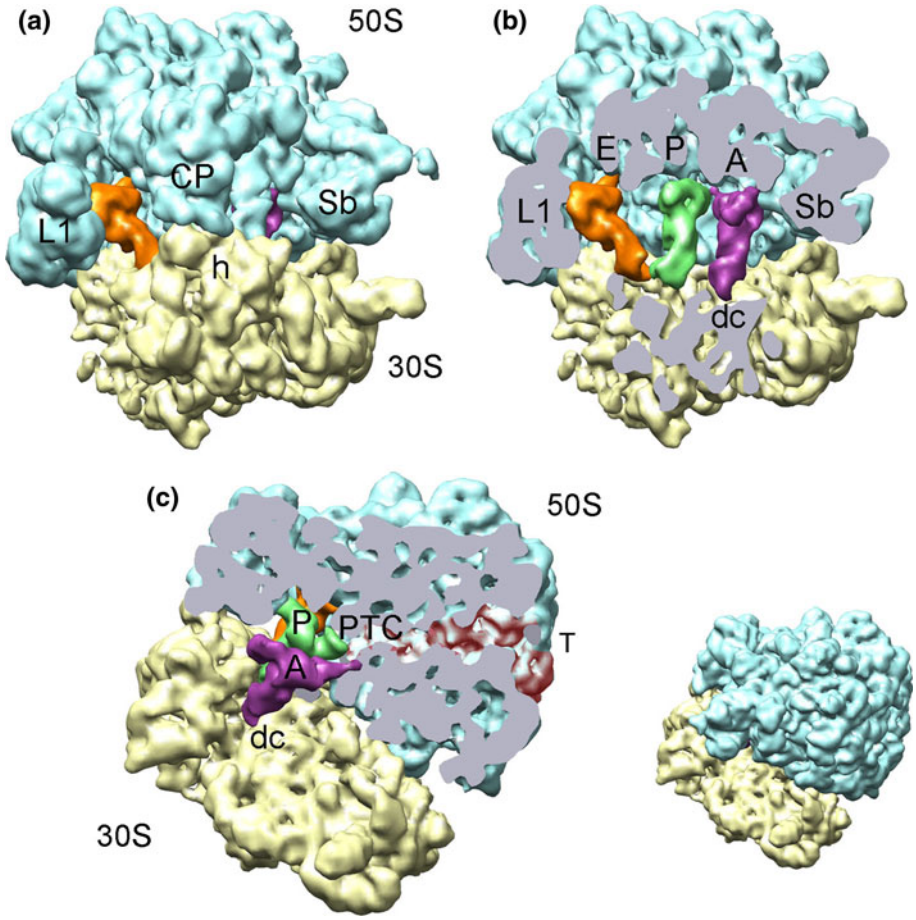

Fig. 2 Rendering of a 3D density map for the *E. coli* 70S ribosome. The large (*blue*) and small (*yellow*) ribosomal subunits (**a**) define an intersubunit space visible in a cutaway depiction (**b**). Here, densities for A- (*magenta*), P- (*green*), and E-site (*brown*) tRNAs are shown. The presence of the polypeptide channel is revealed, crossing the body of the large 50S subunit (**c**). Thumbnail in **c** indicates the orientation of the 70S ribosome. Landmarks and labels: *L1*, stalk of ribosomal protein L1; *CP*, central protuberance; *Sb*, base of the L7/L12 stalk; *h*, head of the small subunit; *dc*, decoding center; *PTC*, peptidyl-transferase center; *T*, peptide tunnel

After accommodation of the incoming aa-tRNA in the A site, rapid and spontaneous peptide bond formation occurs, resulting in ribosomes bearing deacylated tRNA in the P site and peptidyl-tRNA in the A site (Fig. 3). To continue translation following the reading frame of codons in the mRNA, the tRNAs·mRNA complex must proceed through the ribosome moving A- and P-site tRNAs to P and E sites, respectively. Thus, the A site is again vacant and ready to accept the next aa-tRNA. This process is called translocation, and the initial and final ribosomal states are defined as pre- and posttranslocation (Fig. 3). The reaction is catalyzed by the elongation factor G (EF-G), a GTPase.

The universal design of ribosomes, composed of two subunits and the presence of A, P, and E binding sites for tRNAs in both of them, raised an early hypothesis of relative movements between subunits that could promote translocation in one subunit at a time (Bretscher 1968; Spirin 1968). In this model, the tRNAs poise intermediate or hybrid positions different from the classic A, P, and E sites. Two decades later, chemical probing experiments of pretranslocation ribosomes (Moazed and Noller 1989) showed that, after peptidyl transfer and before interaction with EF-G, the tRNAs move spontaneously in the 50S

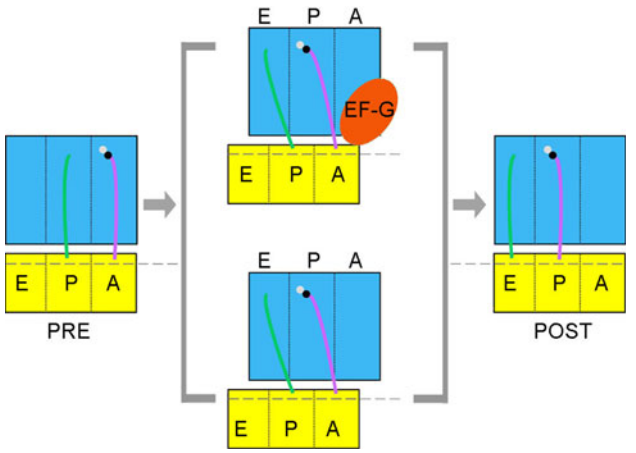

Fig. 3 Model for translocation intermediates. Transition from pre-translocation (PRE) to posttranslocation (POST) ribosomal states involves relative movements between ribosomal subunits and intermediate states for tRNAs. The process is catalyzed by the elongation factor G (EF-G)

subunit, resulting in hybrid P/E and A/P positions for deacylated tRNA and peptidyl-tRNA, respectively. Nonetheless, cryo-EM maps for 70S pretranslocation ribosomes showed tRNAs in classic A, P, and E sites (Fig. 4a), with

no indication of large conformational changes (Valle et al. 2003). The good definition of ribosomal elements and tRNAs in the 3D density map suggested a structurally uniform sample, thus there was no indication of a significant population of translocation intermediates.

The first structural insights into the mechanism of translocation came from the cryo-EM of 70S ribosomes in several complexes with EF-G (Agrawal et al. 1999; Frank and Agrawal 2000; Stark et al. 2000). The data showed a relative rotation between 30S and 50S subunits, a ratchet-like intersubunit reorganization (Frank and Agrawal 2000) that could account for the previously hypothesized structural rearrangements. A similar rotation was described for eukaryotic 80S ribosomes bound to EF2, the eukaryotic counterpart of EF-G (Sengupta et al. 2008; Spahn et al. 2004; Taylor et al. 2007). The poor definition or the absence of tRNAs in the complexes, however, did not provide clear pictures of intermediate or hybrid states. Further characterization of other types of 70S·EF-G complexes provided a more detailed picture of the ribosomal conformational changes (Valle et al. 2003). Using a 70S complex with vacant A site and a deacylated tRNA in the P site, 3D data at a higher resolution ($\sim$10 Å) revealed interesting features of the conformational changes of 70S ribosomal particles associated with EF-G (Fig. 4c, d). The relative rotation between subunits promotes a reorganization of bridges connecting the head of the 30S subunit ("h" in Fig. 4c) and the central protuberance from the 50S subunit ("CP" in Fig. 4c, and comparison between Fig. 4a, b). The direction of movement of the small subunit follows the direction of mRNA and allows the deacylated tRNA to reach the E site in the 50S subunit (Fig. 2d), revealing a hybrid tRNA residing in a P/E position. In the same 3D map, the protuberance at the exit site, the L1 stalk, was seen moving towards the E site, making contact with the tRNA. The combination of rotated 70S ribosomes and the hybrid states for tRNAs converged into an integrated model for translocation. These features were only observed in complexes with EF-G, and pretranslocation ribosomes appeared, at least in the tested conditions, in a nonrotated fashion with tRNAs residing in classic sites (Valle et al. 2003).

Discrepancies regarding the pretranslocation state characterized by cryo-EM and biochemical data were observed in studies using the minimal A-site substrate puromycin (Semenkov et al. 1992; Sharma et al. 2004). The results concluded that pretranslocation ribosomes resided on or sampled intermediate or hybrid states of tRNA binding independently of the action of EF-G, a view confirmed by fluorescence resonance energy transfer (FRET) studies (Ermolenko et al. 2007). Single-molecule

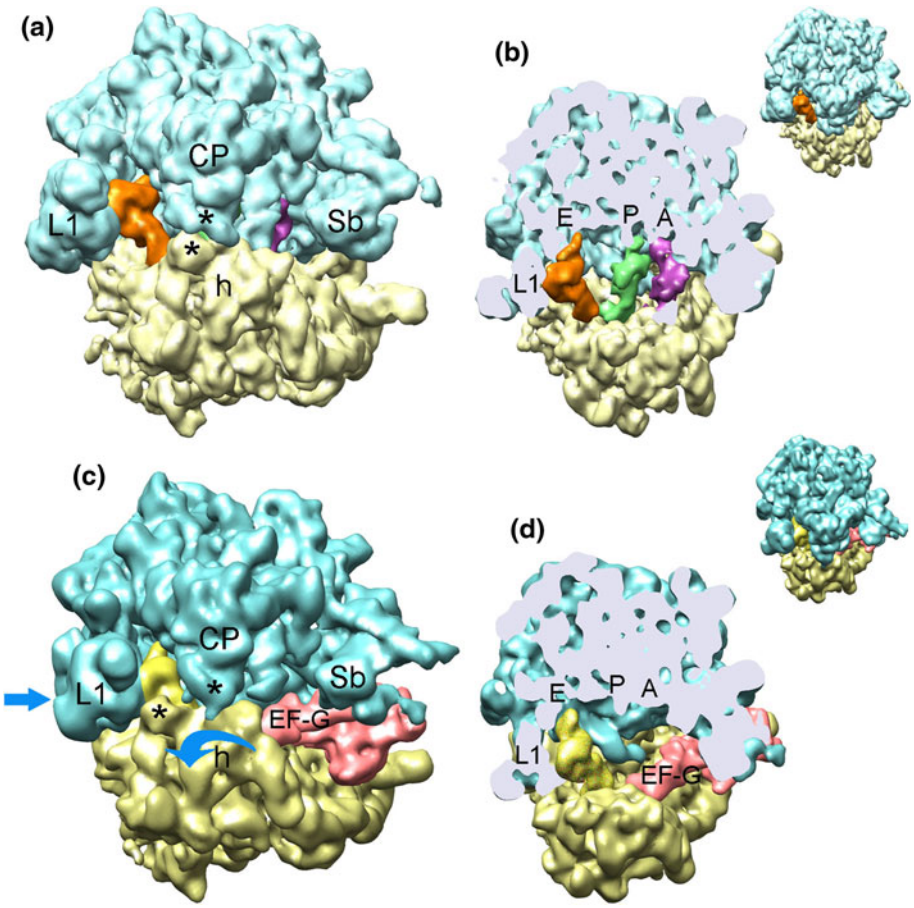

Fig. 4 Cryo-EM maps for 70S ribosomes in pretranslocation state (**a**) and (**b**), and in complex with EF-G and the GTP analog GDPNP (**c**) and (**d**). The pretranslocation 70S shows tRNAs in classic A, P, and E sites. The binding of EF-G to the 70S promotes a relative rotation between subunits clearly observed at the junction between the head (h) and the central protuberance (CP), and the deacylated tRNA is in a P/E hybrid position (**d**). *Asterisks* in **a** and **c** label similar regions on ribosomal subunits. Landmarks as in Fig. 2. Maps fully described in (Valle et al. 2003)

FRET allowed spontaneous fluctuations of single pretranslocation ribosomes between the nonrotated and the rotated states to be monitored, as well as the transitions of tRNAs between hybrid and classic positions in the absence of EF-G (Cornish et al. 2008). It was concluded that intersubunit rotation of the pretranslocation state was thermally driven, and that binding of EF-G stabilized the rotated, hybrid state sampled by the ribosome before the interaction with the elongation factor, in line with earlier footprinting studies (Moazed and Noller 1989).

Dealing with dynamic macromolecules in cryo-EM

Cryo-EM is essentially a 3D averaging technique, thus high-resolution and well-defined structures require uniform populations. This is usually accomplished by chemical synchronization of macromolecular complexes, which ensures homogeneous structural states for the majority of molecules. A dynamic and structurally variable population is a burden, but at the same time it hides valuable information in the sample, and this seemed to be the case for pretranslocation ribosomes. In electron microscopy images, 2D projections are always heterogeneous due to the distinct orientations of the 3D object (Fig. 1), and this variation is intertwined with potential conformational or ligand-binding states. The challenge is not to discriminate between distinguishable projections, but rather to identify 3D objects that produce highly similar 2D images. Thus, conformational changes of the ribosome related to translocation, i.e., the rotated versus the nonrotated states, would produce projections that are difficult to differentiate (several views can be compared in Fig. 5a).

We can find several approaches in the literature on 3D cryo-EM for classification of homogeneous subsets from a mixture. Some straightforward attempts were based on supervised classification (Fig. 5a), where experimental images were compared with projections produced by real (Gao et al. 2004; Valle et al. 2002) or simulated distinct references (Brink et al. 2004). Similarity measurements assign individual images to one of the classes. This approach is limited by prior knowledge of the structural variability and by the potential bias induced by the references. Nonsupervised methods use the combined strategies of 2D alignment, 3D reconstruction, and classification of 3D maps (Elmlund et al. 2010; Fu et al. 2007; Hall et al. 2007; Shatsky et al. 2009), employ a focused classification based on 3D variance calculations (Penczek et al. 2006) or sort subtomograms for macromolecules obtained from random conical tilt-collected data (Sander et al. 2010).

A recently developed method based on likelihood optimization (maximum-likelihood 3D, ML3D) deals with 2D

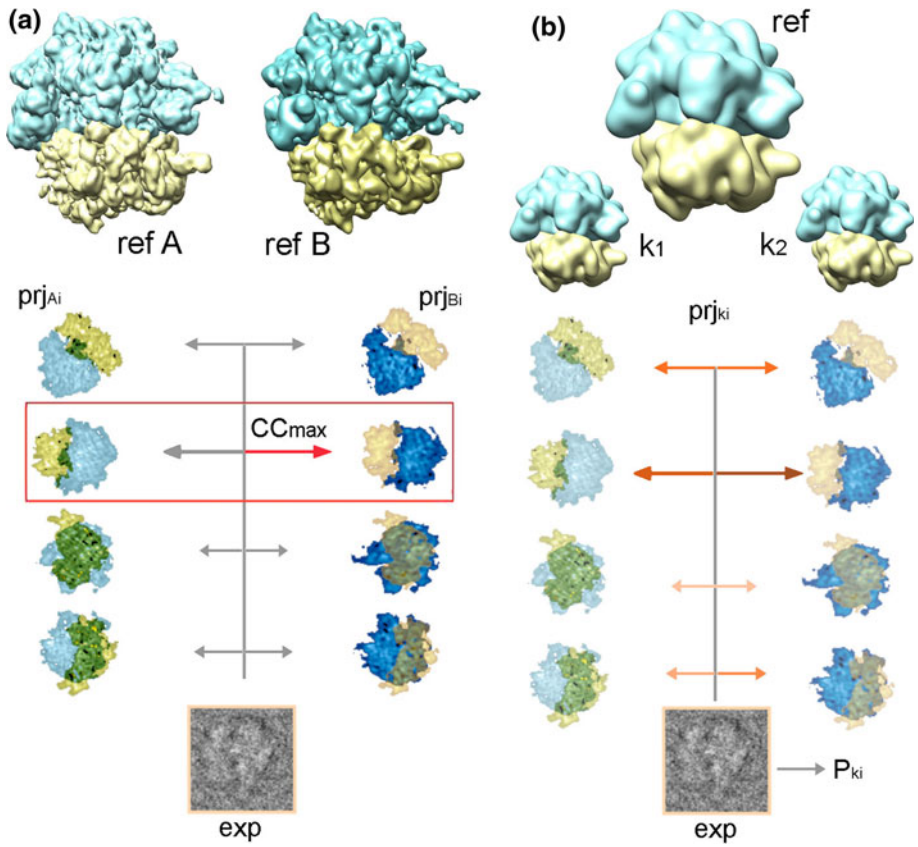

Fig. 5 Schemes for examples of supervised (**a**) and nonsupervised (**b**) strategies for classification used in pretranslocation 70S ribosomes. In the supervised strategy (**a**), the experimental image (exp) is compared with 2D projections coming from distinct initial references (ref) and the maximum cross-correlation (CCmax) dictates the class and the orientation. In ML3D (Scheres et al. 2007), a nonsupervised method (**b**), initial random split of the population generates also two references. The similarity measurements between experimental images and the projections are weighted, all the possibilities considered, and the entire dataset goes through an optimization strategy based on maximum-likelihood algorithms

and 3D variability simultaneously in a nonsupervised manner and with minimum decision-making by the user (Scheres et al. 2007). The procedure looks for a number, *k*, of classes starting by a random split of the population and a common initial reference for the first iteration. The scheme is similar to that of projection matching, except that every assignment is probability weighted (Fig. 5b) and included in a log-likelihood function that will be optimized. Essentially, this is a data-mining procedure that looks for the most probable set of parameters describing the heterogeneous dataset. Initial tests of ML3D with ribosomal samples succeeded in separating EF-G-bound from EF-G-free 70S particles (Scheres et al. 2007).

Pretranslocation ribosomes revisited

In a previous cryo-EM analysis of the pretranslocation state (Valle et al. 2003), 70S ribosomes were seen to be nonrotated with the tRNAs in classic sites. It has to be noted that this 70S map showed density for E-site tRNA. Since the initiator tRNA was still residing in the P site, it was understood that deacylated tRNAs present in the preparation had bound to the E site directly from the solvent side. It was possible that the presence of the tRNA at the E site was blocking the progress of the P-site tRNA toward the P/E position. This fact, together with the line of evidence suggesting the presence of intermediates in the pretranslocation state, motived a revised analysis of this ribosomal complex. Furthermore, the cryo-EM analysis of a probable heterogeneous sample required the use of classification.

New preparations free of spontaneously deacylated tRNAs prone to reach the E site from the solvent were studied. The sample included programmed 70S ribosomes bearing deacylated $tRNA^{fMet}$ in the P site and fMetLeu-$tRNA^{Leu}$ in the A site (Julian et al. 2008). Several experimental conditions were tested, with different combinations of Mg^{++} and spermine (Fig. 6) that were known to modulate the conformation of the ribosome in this step (Kim et al. 2007). In the absence of Mg^{++} ions, the ribosomal

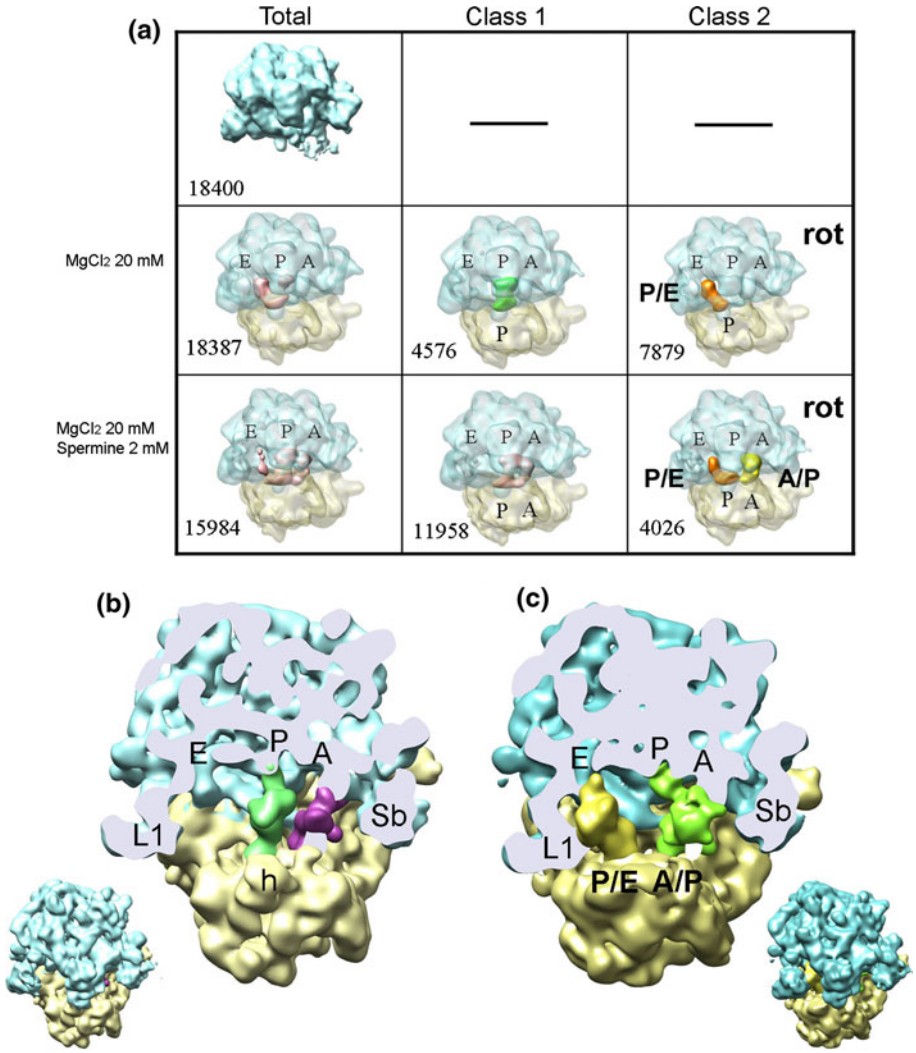

Fig. 6 Cryo-EM analysis of pretranslocation 70S ribosomes. Initial screening for pretranslocation ribosomes at different conditions referred to the presence of Mg^{++} ions and spermine. In the table (**a**), the map for the entire population is shown on the *right*. When ML3D classification was performed, maps for the two separated classes are depicted. Numbers within cells indicate the number of individual images contributing to the depicted map. Semitransparent rendering of ribosomal subunits allows visualization of tRNAs in the intersubunit space. The structural study was scaled up in the conditions favoring a dynamic equilibrium between nonrotated 70S with classic A- and P-site tRNAs (**b**) and rotated 70S ribosomes with tRNAs residing in A/P and P/E hybrid sites (**c**). See (Julian et al. 2008). Landmarks as in Fig. 2

subunits disengage and the cryo-EM map shows the structure of the 50S subunit alone (Fig. 6a). Including Mg^{++} in the preparation preserved the 70S structure, but the cryo-EM maps calculated in the samples with and without spermine (Fig. 6a) depict scattered and incomplete densities for the tRNAs. This was an indication of heterogeneity in the position of the tRNAs in the sample. ML3D classification of both populations revealed the composition of the mixtures. First, class 1 for both sets displayed nonrotated 70S ribosomes, while class 2 showed relative rotation between subunits. The classification of the sample without spermine segregated complexes bearing one single tRNA, a P-site tRNA in the nonrotated 70S, and a P/E hybrid with the rotated 70S. In this condition the A site was not stably bound to the ribosome. In the presence of spermine, the separated classes were grouped between the nonrotated ribosome with tRNAs in classic A and P sites, and rotated 70S with A/P-site and P/E-site tRNAs. Importantly, the initial reference for the ML3D classification was a low-resolution map for the 70S ribosome with no relative rotation between the subunits, thus the classification procedure unveiled conformational changes that had not been included as prior knowledge. Later on, the experiment in the presence of Mg^{++} and spermine was scaled up to improve the resolution of the 3D maps (Fig. 6b, c), confirming that pretranslocation ribosomes can assume either the nonrotated classic state or the rotated hybrid state. In addition, the relative ratio of 70S particles assigned to each state was in agreement with their expected frequencies under the conditions used (Kim et al. 2007). Thus, ML3D classification did indeed efficiently separate the dataset and offered quantitative information about the equilibrium.

Similar results were obtained using a supervised classification of pretranslocation 70S ribosomes from *E. coli* (Agirrezabala et al. 2008), where the total set of images was separated by a comparison with previous maps of 70S ribosomes in the rotated and nonrotated states. The initial references did not contain densities for tRNAs, but the maps after classification showed the corresponding tRNAs in classic and hybrid sites. The good agreement between the results obtained by nonsupervised (Julian et al. 2008) and supervised (Agirrezabala et al. 2008) classifications reinforced the main conclusions, i.e., that translocation in the large subunit can occur before the interaction with EF-G (Fig. 7). The conformational changes are thermally driven, as was later revealed by cryo-EM studies of ribosomal dynamics at different temperatures (Fischer et al. 2010). The binding of EF-G in complex with a GTP nonhydrolyzable analog (GDPNP) shifts the dynamics of the equilibrium to the rotated hybrid state (Cornish et al. 2008), although cryo-EM revealed that domain IV of EF-G overlaps with both A-site tRNA and the A/P hybrid (Fig. 7a). Currently, it is understood that EF-G and GTP hydrolysis by the factor promote the conversion of the ribosome to the nonrotated state and uncouple the movement of the small subunit from that of the tRNAs and mRNA (Taylor et al. 2007). Thus, translocation is accomplished relative to the small subunit (Fig. 7b), and the ribosome again bears a peptidyl-tRNA in the P site, a

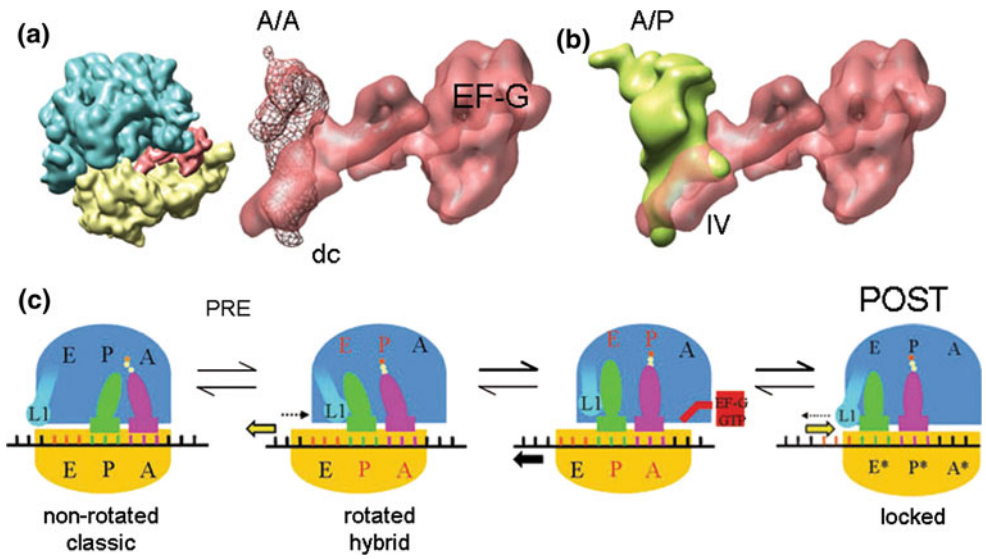

Fig. 7 EF-G in an integrated model for translocation. After the alignment of several cryo-EM maps for 70S and 70S·EF-G complexes, it is clear that EF-G overlaps with the tRNA in A (**a**) or A/P (**b**) site. Currently, it is accepted that pretranslocation ribosomes are in dynamic equilibrium between the nonrotated classic and the rotated hybrid states (**c**). GTP hydrolysis by the elongation factor triggers conformational changes that are coupled to the movement of tRNAs on the 30S subunit, followed by the transition of the 70S ribosome from rotated to nonrotated state. Landmarks as in Fig. 2. Additionally: IV, indicates domain IV of EF-G

condition known to lock the ribosome in the nonrotated classic configuration (Cornish et al. 2008; Valle et al. 2003).

New avenues

The structural characterization of dynamic ribosomes has required implementation of new tools for the classification of heterogeneous populations, and the study of translocation can be seen as a test sample. Recently, using datasets of the order of millions of individual images, nonsupervised classification strategies have revealed the movement of tRNAs through the ribosome, providing a full set of positions and defining a complete trajectory (Fischer et al. 2010). This study took advantage of retrotranslocation, a spontaneous reverse translocation that occurs under certain conditions. As the reaction takes place on the minute timescale, the structural study was carried out in time-resolved fashion, and the kinetic information derived from the cryo-EM work was in agreement with biochemical data. The ability to produce structural and kinetic data from cryo-EM samples is starting to emerge. In the near future, more success stories regarding investigation of structural dynamics by cryo-EM are expected.

Acknowledgments This work is supported by the Department of Industry, Tourism and Trade of the Government of the Autonomous Community of the Basque Country, and the Innovation Technology Department of Bizkaia County.

References

Agirrezabala X, Lei J, Brunelle JL, Ortiz-Meoz RF, Green R, Frank J (2008) Visualization of the hybrid state of tRNA binding promoted by spontaneous ratcheting of the ribosome. Mol Cell 32:190–197

Agrawal RK, Heagle AB, Penczek P, Grassucci RA, Frank J (1999) EF-G-dependent GTP hydrolysis induces translocation accompanied by large conformational changes in the 70S ribosome. Nat Struct Biol 6:643–647

Ban N, Nissen P, Hansen J, Moore PB, Steitz TA (2000) The complete atomic structure of the large ribosomal subunit at 2.4 A resolution. Science 289:905–920

Bretscher MS (1968) Translocation in protein synthesis: a hybrid structure model. Nature 218:675–677

Brink J, Ludtke SJ, Kong Y, Wakil SJ, Ma J, Chiu W (2004) Experimental verification of conformational variation of human fatty acid synthase as predicted by normal mode analysis. Structure 12:185–191

Cornish PV, Ermolenko DN, Noller HF, Ha T (2008) Spontaneous intersubunit rotation in single ribosomes. Mol Cell 30:578–588

Elmlund D, Davis R, Elmlund H (2010) Ab initio structure determination from electron microscopic images of single molecules coexisting in different functional states. Structure 18:777–786

Ermolenko DN, Majumdar ZK, Hickerson RP, Spiegel PC, Clegg RM, Noller HF (2007) Observation of intersubunit movement of the ribosome in solution using FRET. J Mol Biol 370:530–540

Fischer N, Konevega AL, Wintermeyer W, Rodnina MV, Stark H (2010) Ribosome dynamics and tRNA movement by time-resolved electron cryomicroscopy. Nature 466:329–333

Frank J, Agrawal RK (2000) A ratchet-like inter-subunit reorganization of the ribosome during translocation. Nature 406:318–322

Frank J, Zhu J, Penczek P, Li Y, Srivastava S, Verschoor A, Radermacher M, Grassucci R, Lata RK, Agrawal RK (1995) A model of protein synthesis based on cryo-electron microscopy of the *E. coli* ribosome. Nature 376:441–444

Frank J, Penczek P, Agrawal RK, Grassucci RA, Heagle AB (2000) Three-dimensional cryoelectron microscopy of ribosomes. Methods Enzymol 317:276–291

Fu J, Gao H, Frank J (2007) Unsupervised classification of single particles by cluster tracking in multi-dimensional space. J Struct Biol 157:226–239

Gao H, Valle M, Ehrenberg M, Frank J (2004) Dynamics of EF-G interaction with the ribosome explored by classification of a heterogeneous cryo-EM dataset. J Struct Biol 147:283–290

Hall RJ, Siridechadilok B, Nogales E (2007) Cross-correlation of common lines: a novel approach for single-particle reconstruction of a structure containing a flexible domain. J Struct Biol 159:474–482

Julian P, Konevega AL, Scheres SH, Lazaro M, Gil D, Wintermeyer W, Rodnina MV, Valle M (2008) Structure of ratcheted ribosomes with tRNAs in hybrid states. Proc Natl Acad Sci U S A 105:16924–16927

Kim HD, Puglisi JD, Chu S (2007) Fluctuations of transfer RNAs between classical and hybrid states. Biophys J 93:3575–3582

Mitra K, Frank J (2006) Ribosome dynamics: insights from atomic structure modeling into cryo-electron microscopy maps. Annu Rev Biophys Biomol Struct 35:299–317

Moazed D, Noller HF (1989) Intermediate states in the movement of transfer RNA in the ribosome. Nature 342:142–148

Penczek PA, Frank J, Spahn CM (2006) A method of focused classification, based on the bootstrap 3D variance analysis, and its application to EF-G-dependent translocation. J Struct Biol 154:184–194

Ramakrishnan V (2008) What we have learned from ribosome structures. Biochem Soc Trans 36:567–574

Sander B, Golas MM, Luhrmann R, Stark H (2010) An approach for de novo structure determination of dynamic molecular assemblies by electron cryomicroscopy. Structure 18:667–676

Scheres SH, Gao H, Valle M, Herman GT, Eggermont PP, Frank J, Carazo JM (2007) Disentangling conformational states of macromolecules in 3D-EM through likelihood optimization. Nat Methods 4:27–29

Schluenzen F, Tocilj A, Zarivach R, Harms J, Gluehmann M, Janell D, Bashan A, Bartels H, Agmon I, Franceschi F, Yonath A (2000) Structure of functionally activated small ribosomal subunit at 3.3 angstroms resolution. Cell 102:615–623

Seidelt B, Innis CA, Wilson DN, Gartmann M, Armache JP, Villa E, Trabuco LG, Becker T, Mielke T, Schulten K, Steitz TA, Beckmann R (2009) Structural insight into nascent polypeptide chain-mediated translational stalling. Science 326:1412–1415

Semenkov Y, Shapkina T, Makhno V, Kirillov S (1992) Puromycin reaction for the A site-bound peptidyl-tRNA. FEBS Lett 296:207–210

Sengupta J, Nilsson J, Gursky R, Kjeldgaard M, Nissen P, Frank J (2008) Visualization of the eEF2–80S ribosome transition-state complex by cryo-electron microscopy. J Mol Biol 382:179–187

Sharma D, Southworth DR, Green R (2004) EF-G-independent reactivity of a pre-translocation-state ribosome complex with the aminoacyl tRNA substrate puromycin supports an intermediate (hybrid) state of tRNA binding. Rna 10:102–113

Shatsky M, Hall RJ, Nogales E, Malik J, Brenner SE (2009) Automated multi-model reconstruction from single-particle electron microscopy data. J Struct Biol 170:98–108

Spahn CM, Gomez-Lorenzo MG, Grassucci RA, Jorgensen R, Andersen GR, Beckmann R, Penczek PA, Ballesta JP, Frank J (2004) Domain movements of elongation factor eEF2 and the eukaryotic 80S ribosome facilitate tRNA translocation. EMBO J 23:1008–1019

Spirin AS (1968) How does the ribosome work? A hypothesis based on the two subunit construction of the ribosome. Curr Mod Biol 2:115–127

Stark H, Rodnina MV, Wieden HJ, van Heel M, Wintermeyer W (2000) Large-scale movement of elongation factor G and extensive conformational change of the ribosome during translocation. Cell 100:301–309

Steitz TA (2008) A structural understanding of the dynamic ribosome machine. Nat Rev Mol Cell Biol 9:242–253

Taylor DJ, Nilsson J, Merrill AR, Andersen GR, Nissen P, Frank J (2007) Structures of modified eEF2 80S ribosome complexes reveal the role of GTP hydrolysis in translocation. EMBO J 26:2421–2431

Valle M, Sengupta J, Swami NK, Grassucci RA, Burkhardt N, Nierhaus KH, Agrawal RK, Frank J (2002) Cryo-EM reveals an active role for aminoacyl-tRNA in the accommodation process. EMBO J 21:3557–3567

Valle M, Zavialov A, Sengupta J, Rawat U, Ehrenberg M, Frank J (2003) Locking and unlocking of ribosomal motions. Cell 114:123–134

Wimberly BT, Brodersen DE, Clemons WM Jr, Morgan-Warren RJ, Carter AP, Vonrhein C, Hartsch T, Ramakrishnan V (2000) Structure of the 30S ribosomal subunit. Nature 407:327–339